The Importance of Anisotropy for Prestack Imaging

Xiaogui Miao*, David Wilkinson and Scott Cheadle
Veritas DGC Inc., 715-5th Ave. S.W., Calgary, AB, T2P 5A2 Calgary, AB
Xiaogui_Miao@veritasdgc.com

Bruce Ver West and Phil Hilton
Veritas DGC, 10300 Town Park, Houston, TX 77072 USA

ABSTRACT

Introduction

The presence of anisotropy in the subsurface is a generally accepted but commonly overlooked concept in processing. When it is addressed, usually only the effect on moveout is considered. This paper shows the importance of including anisotropy in imaging, not only because it properly handles the long offset moveout but also because it correctly handles the focusing and spatial positioning which is subtler but may be even more important. The paper shows an imaging problem from the coast of the Gulf of Mexico. It is a problem involving fault related rollover structures that are common worldwide. The fundamental aspects of anisotropy in imaging are introduced. Then the impact of anisotropic prestack time migration on this example is shown along with a practical strategy for its implementation. The impact is demonstrated using sections and time slices from the 3D survey comparing previous processing without anisotropy to new processing with anisotropy. The anisotropic prestack time migration better focuses and images the complex growth fault structures and leads to significantly higher spatial resolution of the targets. With an initial estimate of anisotropy parameters from time imaging, the potential for further imaging improvements using prestack depth migration are also considered.

Anistropic Prestack Time Imaging

In prestack time imaging there are two forms of anisotropy. The first is an effective anisotropy, which is the result of ray bending due to vertical variations in the interval velocity. The second is the intrinsic anisotropy of the subsurface. In this paper we consider only the case of vertical transverse isotropy (VTI). The following equation is a modified formula for the traveltime for each leg (source or receiver) of the double square root traveltime equation in the prestack time migration.

$$t_\rho^2 = t_0^2 + \frac{x^2}{v_2^2} - \frac{2\eta_v x^4}{v_2^2[t_0^2 v_2^2 + C_v x^2]} - \frac{2\eta x^4}{v_2^2[t_0^2 v_2^2 + C x^2]}, \quad \eta_v = \frac{1}{8}\left[\frac{v_4^4}{v_2^4} - 1\right]. \quad \text{(Eqn. 1)}$$

Here v_2 is the rms velocity (second moment of the interval velocity), v_4 is the fourth moment of the interval velocity, x is the distance from image point to

source or receiver and t_0 is the one way image time. The first two terms of this equation give the straight ray traveltime. The third term is an approximation for the additional effect of ray bending on the traveltime. The fourth term adds the effect of intrinsic anisotropy where η is related to the RMS intrinsic anisotropy (Tsvankin and Thomsen, 1994). The constant C in the fourth term can be either $C = 1 + 2\eta$ or $C = 1$ (Grechka, 1998). Either choice gives a similar result in the limit of small η since there is already a factor of η in the numerator. The effective anisotropy, η_v, from the ray bending is calculated from the velocity profile according to Taner and Koehler (1969). It gives a well-defined contribution to the traveltime for the 4th order but adding a 4th order term to the straight ray expression results in an expression for the traveltime which diverges for large offsets. Adding the C_v in the denominator results in a rational approximation which modifies the 2nd order term for large offsets. Various choices can be made for C_v. One can choose it so the 6th order term is preserved. However, this also can result in a divergence in the traveltime for some velocity profiles. Another choice is to use the same form as for the intrinsic anisotropy term. This choice results in the effect of the ray bending anisotropy being prematurely damped at intermediate offsets. A better choice, which is employed here, is to optimize C_v such that it is stable and yields a good approximation to the 6th order term and the ray-traced result. Simply adding the ray bending anisotropy to the intrinsic anisotropy in the last term (or treating it as one effective anisotropy) is not correct since the two effects have different points where they make the transition from their small offset limits to their asymptotic limits.

Growth Fault Example

The problem of imaging dipping events and faults in growth fault structures in the Gulf of Mexico will be used to illustrate the importance of anisotropy in prestack imaging. Figure 1 shows a section from a straight ray 3D prestack time migration of an extensional fault block. There is significant rotation of the beds in the fault block while the events above and below are relatively flat. The RMS migration velocities for the events above and below this fault block are in the range 9500-9900 ft/s. However, these velocities result in significant under-migration of the dipping events in the fault block. The dipping events are imaged in a more correct location at a velocity of 10,900 ft/s, but such a velocity would result in degradation of the glide plane and the events immediately below the fault block. Analysis of the gathers shows anisotropy of about □=0.02 at 1.5 sec. but data quality and offset limitations prohibit such analysis below 2.0 sec. This does not mean that anisotropy is non-existent below 2.0 sec. It also does not mean that the imaging process is insensitive to anisotropy below 2.0 sec. While the effects of anisotropy cannot be seen in the gathers (either pre-migration or post-migration), anisotropy is still affecting the imaging of dipping reflectors even for small offsets.

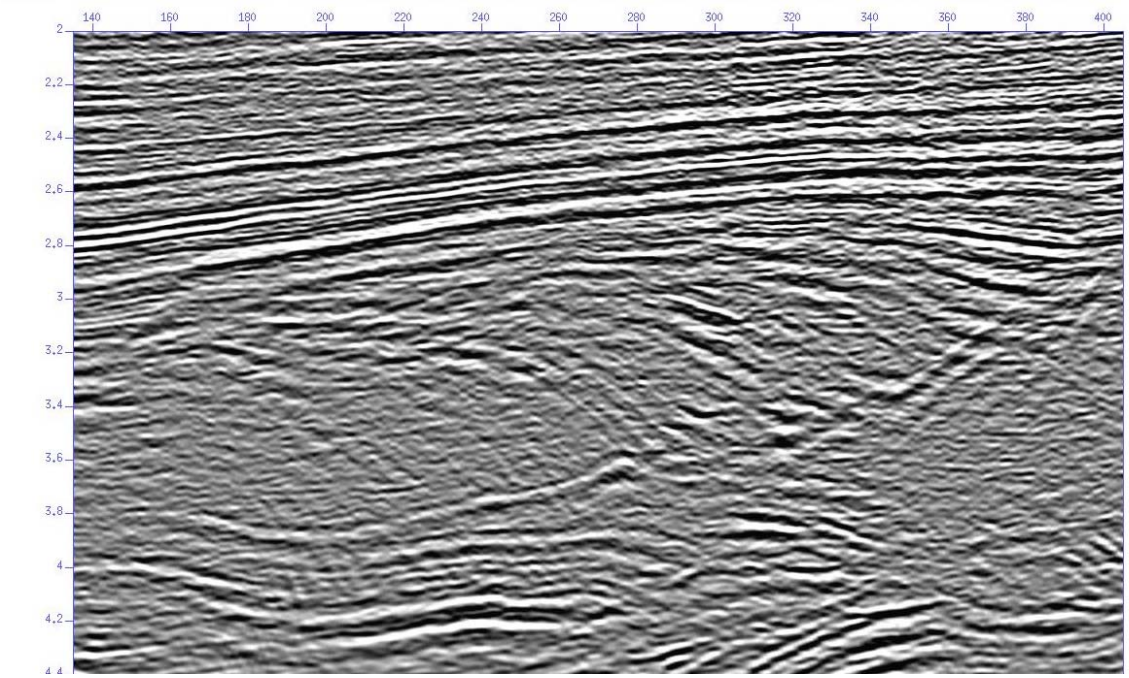

Fig. 1: Prestack time migration using straight rays.

Figure 2 shows the same section after 3D prestack time migration with a curved ray approximation as discussed above. While it has sharpened some of the dipping events in the fault block, they are still significantly under-migrated. The ray bending anisotropy at this level is only $\eta_v = 0.015$ which is significantly less than is needed to explain the apparent migration velocity differences between the flat and dipping events.

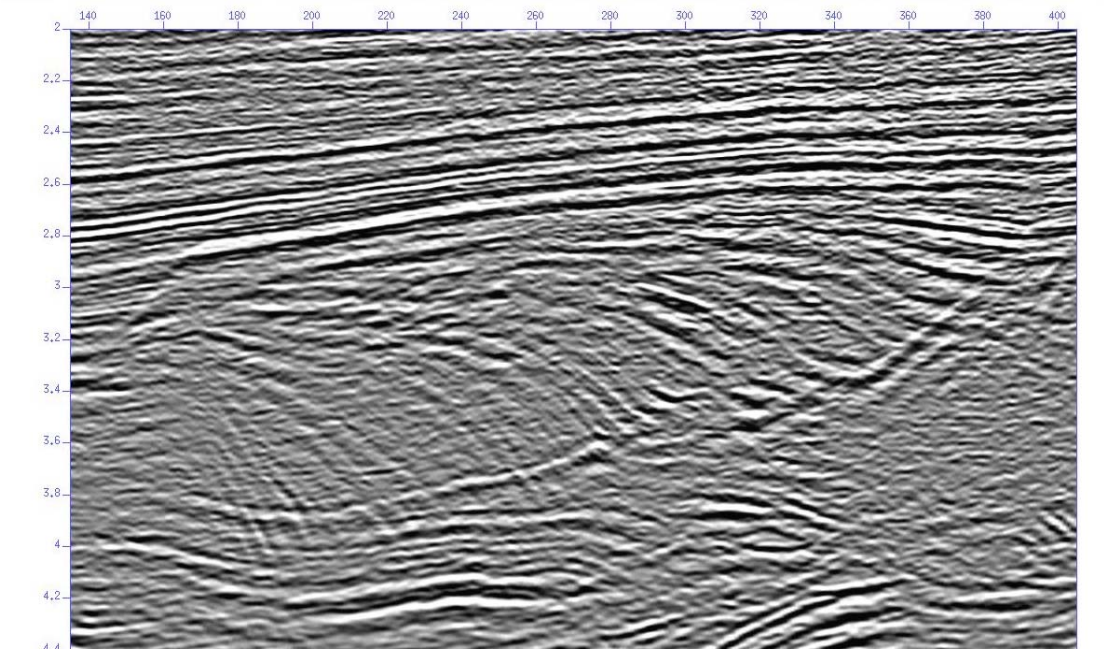

Fig. 2: Prestack time migration using curved rays.

The intrinsic anisotropy parameter was then scanned for values between □=0.02 and 0.10. The value of 0.06 gave the 3D anisotropic curved ray prestack time migration shown in figure 3. The VTI assumption made in the traveltime computations is considered applicable here since the anisotropy is generated by the gently dipping sand-shale sequences above the target. The more steeply dipping events in the fault block are now migrated into the block optimally in the time domain while the events above and below remain well imaged. In addition the fault plane is better imaged on the right side of the section both in terms of its position and its amplitude. This improvement in fault plane imaging can be seen throughout the volume. In the results shown in figures 1-3, the migration velocity was held fixed and was smoothly varying from 9,500 ft/s just above the fault block to 9,900 ft/s just below it. A final anisotropic curved-ray prestack time migration was done using a single time varying □ profile chosen based on the observed non-hyperbolic moveout in the shallow section and the results of the□ imaging scans in the deeper section. Thus, using anisotropic curved-ray prestack time migration, we were able to better image the events from dipping beds, subhorizontal strata and fault planes in and around the fault block with a very smooth velocity model and a smooth □ profile Figure 4 shows a time slice through the 3D volumes of the straight ray and anisotropic curved ray prestack time migrations. The time slice was made at 3300 ms. which cuts through the fault block. The dramatic improvement in the spatial resolution of the anisotropic result comes from the improved imaging of the dipping events.

Anisotropic Prestack Depth Migration

Prestack depth migration is the natural extension to time domain imaging. In the previous section the distinction is made between effective anisotropy due to ray bending and intrinsic anisotropy as a rock property. The first two terms in eqn. 1 approximate the travel time effect of a curved raypath through a V(z) gradient. In prestack depth migration, ray bending is handled directly by calculating travel times based on explicit ray tracing through a model representing a spatially varying interval velocity field. The intrinsic anisotropy term in eqn. 1 is an RMS type value applicable for the case of vertical transverse isotropy, or VTI. Although implementation of VTI anisotropy in the time migration has improved the imaging of dipping layers with the fault block, the gentle dip of the overlying anisotropic strata suggests that TTI or tilted anisotropy may produce even better results. Recent modeling by Vestrum (2002) has demonstrated that reflection point smearing due to anisotropy is surprisingly large at low tilt angles from the vertical of the symmetry axis. The extent to which the anisotropic imaging responds best to the VTI or TTI model will depend on whether the symmetry is controlled by fabric related to a vertical compaction gradient or bedding dip. The η=0.06 from the time migration may be used as an initial estimate of the anisotropy parameters for depth model building, since under the weak anisotropic assumption, $\eta \approx \varepsilon - \delta$ (Grechka, 1998). Models incorporating VTI and TTI assumptions are being tested using a new 3D anisotropic prestack depth

migration developed for parallel computation of travel times and imaging using large scale PC clusters. Results comparing the VTI time domain imaging and VTI and TTI model-based prestack depth images will be discussed.

Conclusions

Including the effects of anisotropy in imaging is important not only because it properly handles the long offset moveout but also because it correctly handles focusing and spatial positioning. The latter effect is frequently overlooked in anisotropy analysis. The example of the rollover associated with deep extensional faults shows that anisotropy can be important and easy to include in prestack time imaging even when it is not manifested in the long offset moveout. The anisotropic prestack time migration better focuses and images the conflicting dip of complex growth fault structures in the time domain and leads to significantly higher spatial resolution of the targets, which also provides a fast and economic solution for anisotropic imaging. Anisotropic prestack depth migration is evaluated for further improvement of the focusing of the events and imaging of the complex fault systems in this example.

References

Grechka, V. Y., 1998, Transverse isotropy versus lateral heterogeneity in the inversion of P-wave reflection times, Geophysics, **63**, 204-212.
Taner, M. T., and Koehler, F., 1969, Velocity spectra-digital computer derivation and applications of velocity functions, Geophysics, **34**, 859-881.
Tsvankin, I., and Thomsen, L., 1994, Nonhyperbolic reflection moveout in anisotropic media, Geophysics, **59**, 1290-1304.

Vestrum, R., 2002, 2D and 3D Anisotropic depth migration case histories, SEG International Exposition Extended Abstracts

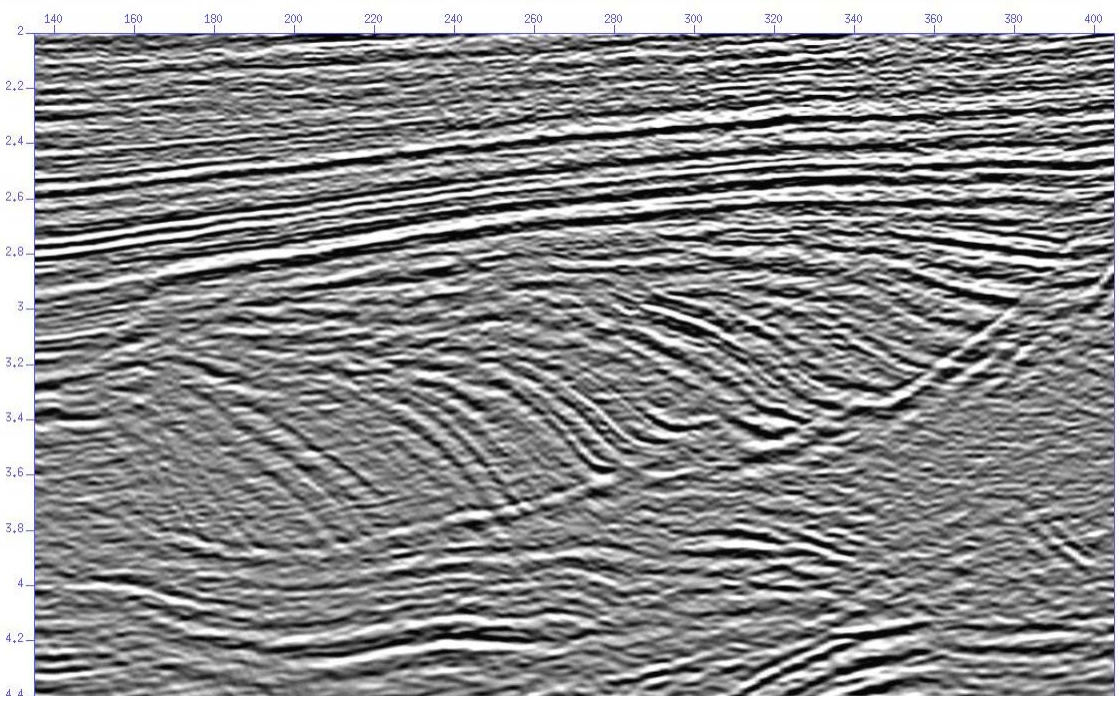

Fig. 3: Anisotropic prestack time migration using curved rays with η=0.06.

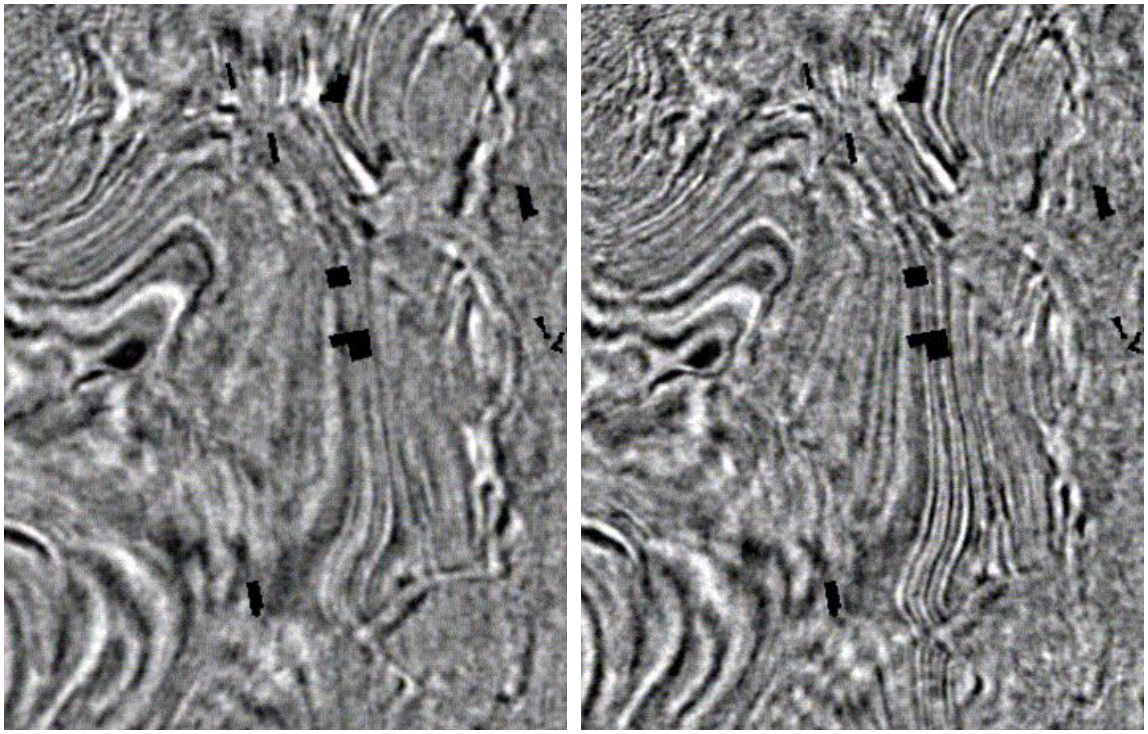

Fig. 4: Comparison of time slices at 3300 ms of the final 3D prestack time migration using straight rays (left) and anisotropic curved rays (right). The fault block shown in Figures 1-3 is in the middle of these time slices and the dashed line gives the location of the sections.